

Foaming Poly(vinyl alcohol)/Microfibrillated Cellulose Composites with CO₂ and Water as Co-blowing Agents

Na Zhao,^{†,‡} Lun Howe Mark,[‡] Changwei Zhu,[‡] Chul B. Park,^{*,‡} Qian Li,^{*,†} Robert Glenn,[§] and Todd Ryan Thompson[§]

[†]National Engineering Research Center for Advanced Polymer Processing Technology, Zhengzhou University, Zhengzhou 450002, China

[‡]Microcellular Plastics Manufacturing Laboratory, Department of Mechanical and Industrial Engineering, University of Toronto, Toronto, Ontario, Canada, M5S 3G8

[§]Beauty Technology Division, Procter and Gamble Company, Mason, Ohio 45040, United States

ABSTRACT: We investigated the continuous extrusion foaming of poly(vinyl alcohol) (PVOH)/microfibrillated cellulose (MFC) composites using supercritical carbon dioxide (scCO₂) as the blowing agent. First, the as-received PVOH pellets were compounded with water to decrease their melting point. Then, they were compounded with an MFC solution to prepare the sample. Both scanning electron microscopy (SEM) and environmental scanning electron microscopy (ESEM) showed that the MFC dispersed well in the PVOH/MFC composites. Differential scanning calorimetry (DSC) results showed that adding MFC affected the thermal behavior. This, in turn, affected cell nucleation and cell growth phenomena during foam extrusion. Water also acted as a co-blowing agent, together with scCO₂, in creating biodegradable polymer foams with a uniform cell structure and a high cell density. The effects of the MFC content, scCO₂ content, and die temperature variations on the cell density and cellular morphology of the PVOH/MFC composite foams were examined systematically.

INTRODUCTION

Environmental concern about plastic waste disposal has grown. Thus, more attention has been placed on a product's life cycle and its end-of-life disposal and on the use of natural fibers and biodegradable polymers.¹ Microfibrillated cellulose (MFC) has generated great interest as a microsize/nanosize filler, because of its high aspect ratio, high stiffness, strength, and biodegradability.^{2–5} Moreover, like wood/natural fibers,^{6–8} MFC is hydrophilic, which means it provides a stable solution when used with water. Consequently, MFC-water-soluble polymer composites were created by melt mixing MFC suspensions to produce a homogeneous dispersion of MFC in the polymer matrix.^{9,10}

As an important water-soluble and biodegradable polymer, poly(vinyl alcohol) (PVOH) has several advantages. These include its compatibility with many organic and inorganic materials, its good ion exchange, chelation, physical adsorption and its polarity. Thus, environmentally friendly PVOH foams have many potential applications. They can be used to make surgical accessories. They can also be used in drug delivery, packaging, heavy metal ions adsorption, and in acoustic noise reduction.^{7,11,12} Because of multihydroxyl group interactions, PVOH has strong intermolecular and intramolecular hydrogen bonding. Such strong bonding causes the melting temperature of PVOH to be very close to its decomposition temperature, and this can potentially lead to thermal degradation during extrusion processing.¹¹ To prevent this from happening, plasticizers are added as processing aids.

Glycerol is a commonly used plasticizer during PVOH processing. It can permanently decrease the melting temperature of PVOH/glycerol compounds, because it remains within the PVOH matrix without evaporating under ambient storage

conditions. However, glycerol has several drawbacks. It tends to migrate out of the finished product and causes an undesirably sticky product surface. In addition, glycerol-plasticized PVOH products tend to harden during storage. This is because the high mobility of PVOH chains leads to PVOH crystallization, and crystallization in the PVOH matrix can expel extra glycerol. This can result in geometrically deformed final products. Therefore, glycerol may not be a suitable choice to produce consistently molded PVOH products.¹³ Amphemicols, which represent another type of plasticizer, have a high boiling temperature, which interfere with the PVOH processing temperature, making them unsuitable for use. Fortunately, water is a highly suitable plasticizer for PVOH thermal processing, because it can increase the flexibility of the PVOH chains without destroying the hydrogen bonding and without causing phase separation.^{14–16} In addition, water is an economic and environmentally friendly blowing agent (BA).¹¹

The reported advantages of microcellular foamed plastics include their higher impact strength,¹⁷ higher toughness,¹⁸ increased fatigue life,¹⁹ and their better light-reflecting properties.²⁰ This has been in comparison to their solid counterparts. The addition of fine natural fibers improves their foaming behavior.²¹ Also, as the fiber size decreases, their composite properties improve.²² Despite these advantages, many challenging obstacles remain in the production of well-dispersed fiber composites and their foams. This is especially so for those with fine and high-aspect-ratio fibers.

Received: May 17, 2014

Revised: June 30, 2014

Accepted: July 9, 2014

Published: July 9, 2014

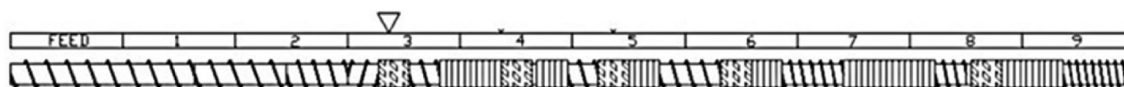


Figure 1. Schematic of the screw configuration of a twin screw extruder.

Several researchers have studied PVOH and its composite foams. Thermoplastic PVOH foams have been obtained with methanol, water, and a cross-linking agent to achieve lower density foams using a twin-screw extruder.^{23,24} Water has also been used as a plasticizer and a BA to produce PVOH foams in extrusion, with talc and CaCO_3 added as nucleating agents.¹¹ PVOH foams and their composites have also been made by mechanically stirring a PVOH solution with and without fillers and by using liquid nitrogen to freeze the cell structure.^{7,25} Batch foaming of PVOH reinforced with nanofibrillated cellulose has also been done to develop a cellular structure. This has been accomplished by inducing thermodynamic instability in dissolved CO_2 in the PVOH matrix at the point of supersaturation with a rapid solubility drop.²⁶

In this study, we used supercritical (sc) CO_2 as the main BA in continuous extrusion to achieve PVOH/MFC composite foams with a uniform cell structure and a high cell density. Water acted as a plasticizer and a co-BA. It would be quite difficult to achieve microcellular PVOH/MFC composite foams with a high cell density using water alone, because of the low thermodynamic instability induced by the pressure drop. This is because water has a strong affinity with PVOH, and thus it is highly soluble in it. On the other hand, scCO_2 has been effectively used to induce a microcellular structure, because of its relatively low solubility in PVOH.²⁶

The water that was dissolved in the PVOH was expected to increase the CO_2 's solubility, because of the swelling of the PVOH.^{27,28} Yet, it seems exceedingly difficult to measure the solubility of CO_2 in PVOH/water or PVOH/MFC/water systems using any of the current state-of-the-art technology (e.g., the pressure decay method^{29,30} or the gravitational method that is based on the magnetic suspension balance^{31,32}), because water evaporates during the solubility measurement. Thus, the increase in the CO_2 solubility in the PVOH or in the PVOH/MFC mixtures cannot be quantitatively measured as a function of water content.

Foaming in continuous extrusion and injection molding tends to have much less cell density, compared with batch processes that distribute the same nucleating agent (and the same content) in the same polymer matrix, and which dissolve the same BA (and the same content). We believe that the thermodynamic instability generated in extrusion and injection molding is much lower than it is in batch processing, because the melt in extrusion and injection molding has lower viscosity and elasticity. This results in lower stress variations around the nucleating agents (or the filler particles used in this research),^{33–35} which create a larger critical radius. This, in turn, causes lower cell nucleation rates.^{36,37} Because of their pliability, nanosize thin fibers might not create large stress variations. In other words, the generated compressive and tensile stresses around the fibers will quickly relax because of their deformity, and lower cell nucleation rates will result.³⁵ It often happens that well-exfoliated nanoparticles do not participate in cell nucleation, and only the rigid intercalated nanoparticles cause cell nucleation in nanocomposite foams.³⁵ However, with the creation of crystals along the fibril surface, the well-dispersed fibrils (or exfoliated nanoparticles) decrease

their pliability and become sufficiently rigid to create larger stress variations. This, in turn, can cause the thin fibrils to participate in cell nucleation by reducing the critical radius around them. Consequently, cell density will be increased. In other words, not only the added MFC fibrils themselves, but also the crystals that develop around them can play a critical role in PVOH/MFC composites foaming. Therefore, the crystallization behaviors of the PVOH/MFC composites are important to understanding their foaming behaviors. In this context, we have studied the effects of fiber content and processing parameters on crystallization kinetics, cell morphology, and cell density.

EXPERIMENTAL PROCEDURE

Materials. The microfibrillated cellulose used in this study was industrial-grade KY100G (supplied by Daicel FineChem Ltd.). The MFC was obtained in the form of an aqueous suspension. The MFC fibers ranged in width, from 10 nm to 15 μm , and length, from 0.1 μm to several micrometers.

Poly(vinyl alcohol) (Mowiol 23-88) was supplied by Kuraray Company. Mowiol 23-88 is a partially hydrolyzed grade (86.7–88.7 mol %) with the weight-average molecular weight of 150 000 g/mol and has a density of 1.3 g/ cm^3 at 20 °C. Carbon dioxide (99.98% of purity), supplied by Linde Gas, was used as a physical BA. The PVOH and MFC were used as received, without any additional processing aids.

Experimental Setup and Procedure. A co-rotating twin-screw extruder (Leistritz Corporation, $D = 27$ mm, $L/D = 40$) was used in compounding PVOH with water or with an MFC solution. The screw configuration, as Figure 1 shows, was designed to provide both dispersive and distributive mixing. As a plasticizer, water was injected into the PVOH melt at zone 3. To create PVOH/MFC composites, a 0.5 wt % MFC solution (as suggested by Daicel FineChem, Ltd., to achieve a good MFC dispersion), was metered in at zone 3. PVOH/MFC composites with MFC contents of 0.25 and 0.5 wt % were created by using different metering rates. Table 1 lists the temperature profile of the twin-screw extruder. After the compounded extrudate exited the die, it was air-cooled, and

Table 1. Temperature Profile of a Twin Screw Extruder during PVOH/Water Compounding

parameter	value
feeding temperature, T	
zone 1	150 °C
zone 2	200 °C
zone 3	220 °C
zone 4	210 °C
zone 5	190 °C
zone 6	180 °C
zone 7	170 °C
zone 8	155 °C
zone 9	150 °C
die	140 °C
speed/rpm	100 rpm

then fed into a pelletizer to make pellets of PVOH/water or PVOH/MFC composites.

PVOH/water and PVOH/MFC composites extrusion foaming experiments were conducted in a small tandem line system with the amount of water being 22.2 and 12.5 wt %, respectively. Table 2 lists the temperature profile of the first

Table 2. Temperature Profile of First Extruder in the Small Tandem Line during Foaming

first extruder	temperature, T (°C)
zone 1	70
zone 2	165
zone 3	195
zone 4	195
zone 5	185

extruder of the small tandem line system. The initial temperatures of the second extruder and of the filamentary die were each set at 180 °C. Then scCO_2 was injected into the first extruder and dissolved into the PVOH/water and PVOH/MFC composites melt. The die temperature was decreased at an interval of 5 to 140 °C. PVOH/MFC composite extrusion foaming experiments were conducted with 5, 7, and 9 wt % scCO_2 and with 0, 0.05, and 0.1 wt % MFC.

It was observed that feeding PVOH pellets with a high water content (e.g., 30 wt % water) into the hopper was not steady and that the pressure fluctuated. Because of water evaporation from the PVOH pellets during melting, the water vapor came

out (through the solid bed) to the hopper. The pellets in the hopper became wet, and it was relatively hard to achieve a stable feeding of these materials. Feeding became easier with a higher rotational screw speed. This was most likely because less water evaporated from the PVOH pellets during the reduced residence time. The feeding of PVOH pellets could be done by using a twin-screw extruder with a positive displacement pumping nature. However, we conducted the single-screw extrusion foaming experiments using PVOH pellets with a relatively lower water content to ensure a stable extrusion condition. We collected the samples only after a steady state had been reached under each processing condition.

Foaming Characterization. To analyze the cellular morphology, the foamed samples were dried and cut using a razor blade. The cryo-fracture employing liquid nitrogen was not used, because of the condensed water droplets that appeared on the sample (and tools) when they were exposed to ambient air and dissolved the foam samples. Next, the cross section of the foam was coated with a thin layer of platinum, using a sputter coater.

The microstructure was then examined using a scanning electron microscopy (SEM) system (Model JSM-6060, JEOL). The regular SEM equipment typically requires a vacuum, so the PVOH samples were dried before the SEM experiments. Because of the shrinkage and potential rupture of the cell opening that can occur during drying, the original morphology might not have been visible in the dried PVOH samples. Therefore, an environmental scanning electron microscopy

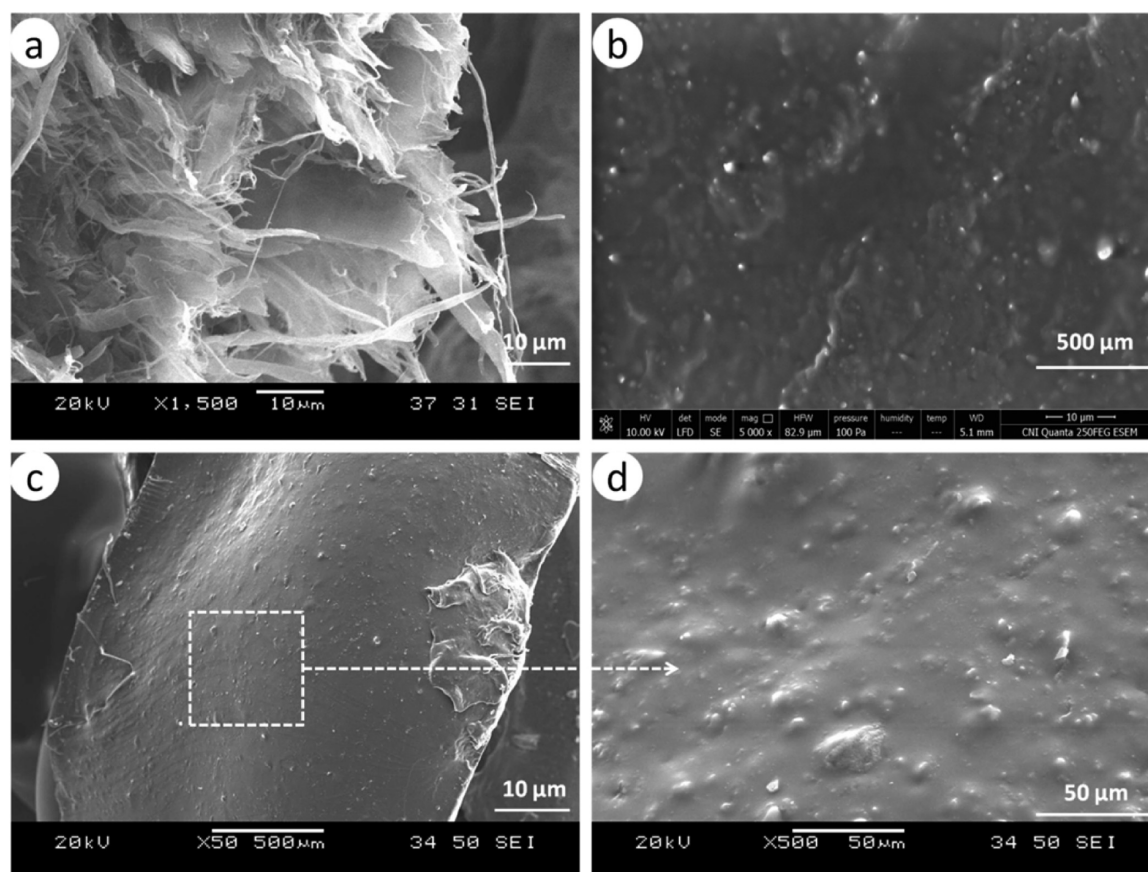


Figure 2. (a) SEM image of microfibrillated cellulose, (b) ESEM image of PVOH/MFC composite, and (c and d) SEM images of PVOH/MFC composites at low and high magnification.

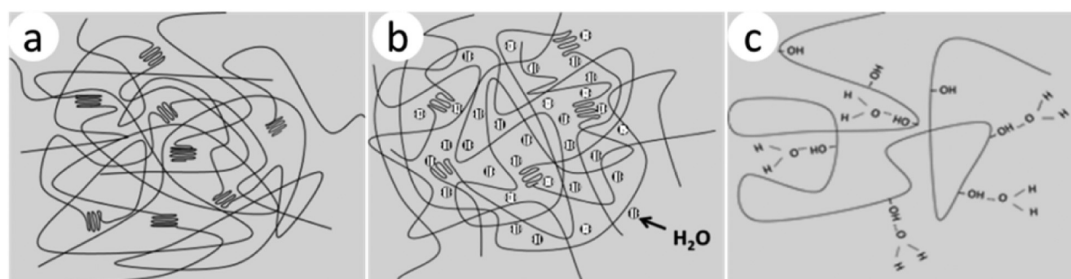


Figure 3. (a) PVOH semicrystalline structure, (b) water effect the PVOH semicrystalline structure, and (c) hydrogen bonding between water molecular and PVOH chains.

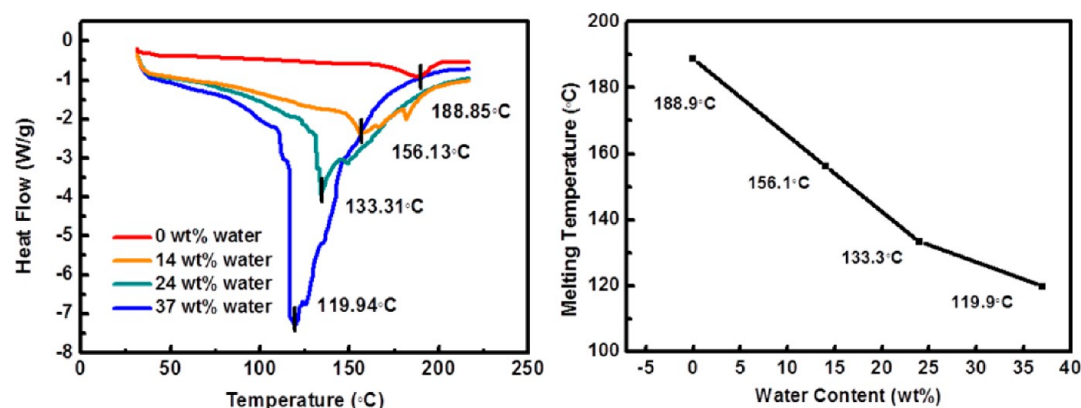


Figure 4. DSC thermograms showing the melting temperature at various water contents in PVOH.

(ESEM) system (Quanta FEG 250) was also used in the structural characterization.

The expansion ratio (Φ) was evaluated using a water-displacement technique based on the ASTM Standard D792-00. We analyzed the SEM micrographs and measured the average cell sizes. The average cell densities were then calculated using eq 1:

$$\text{cell density} = \left(\frac{nM^2}{A} \right)^{3/2} \times \Phi \quad (1)$$

where n is the number of cells in the micrograph, and A and M are the area and magnification factor of the micrograph, respectively.

RESULTS AND DISCUSSION

1. MFC Distribution in PVOH. In extrusion processing, well-dispersed MFC in PVOH is vital to producing fine-celled PVOH/MFC composite foams. Figure 2a shows a SEM image of the dried MFC film under high magnification. It was found that multiple MFC fiber sizes contained nanofibrils, fiber fragments, and fibers, all of which have strong hydrophilic characteristics in water. The hydroxyl groups of the anhydroglucose units in MFC and water-plasticized PVOH produce hydrogen bonding, because of the interactions of PVOH/MFC blends.⁹ Thus, water-soluble PVOH that is compounded with a stable MFC suspension by using a twin-screw extruder becomes easily processable. Figures 2c and 2d show the distribution of MFC in PVOH when tested with a higher MFC loading (0.75 wt %). The white dots are small MFC fibrils that were distributed throughout the PVOH matrix. These, and similar results, were reported by ref 10. Figure 2b

also shows the distribution of MFC in PVOH using environmental scanning electron microscopy (ESEM).

2. Thermal Behaviors of PVOH and PVOH/MFC Composites. **2.1. Effect of Water on the Thermal Behavior of PVOH.** Water can be quickly absorbed in partially hydrolyzed PVOH. Figure 3 schematically shows the effect of water on PVOH chains. Because of its small molecular volume, water can easily penetrate the amorphous area and also some crystalline areas of PVOH,³⁸ as Figure 3b shows. In such close contact, the oxygen atoms on the water molecules connect with the hydrogen atoms on the hydroxyl groups of PVOH chains. The hydrogen bonding between the hydroxyl groups and the water will disrupt the intermolecular and intramolecular bonding that occurs in the PVOH chains, as shown in Figure 3c. This disruption can increase the distance between the PVOH segments, dissolve small and imperfect crystals, and reduce the overall crystallinity.

The melting behavior of PVOH/water compounds with different water content and PVOH/MFC composites were investigated using differential scanning calorimetry (DSC) (Model Q2000, TA Instruments). The compounded samples were characterized using a temperature that ramped from 30 °C to 230 °C with a heating rate of 10 °C/min. Figure 4 shows the effect of water on the PVOH/water compounds. With the addition of water, the melting temperature (T_m) of the PVOH decreased sharply, because of the increased PVOH chain mobility. For instance, when the water content was 14 and 37 wt %, the melting temperature of the PVOH/water compound was 156 and 120 °C, respectively, indicating that water as a plasticizer increased the processing window. These results are consistent with earlier ones.¹¹ However, it should be stated that, in this DSC experiment, the decreased melting temperature is underestimated. Because of the sample's unavoidable

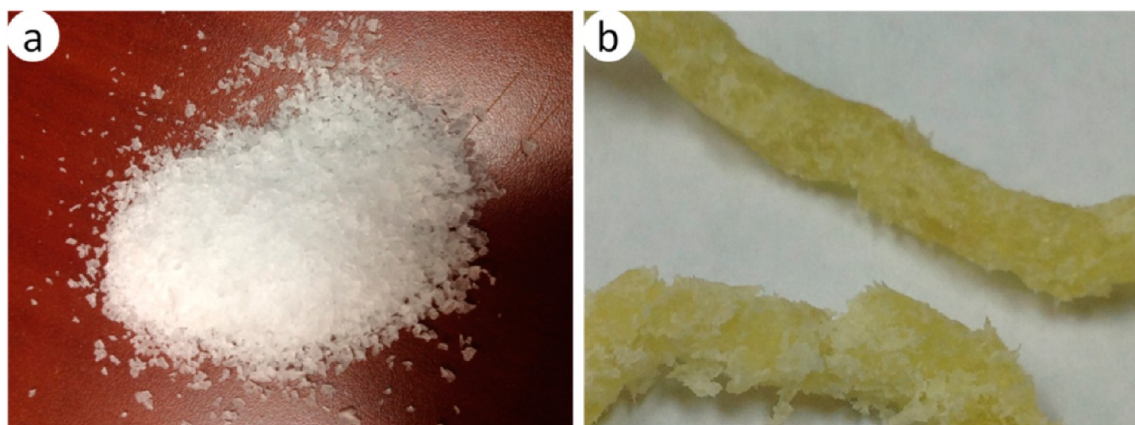


Figure 5. (a) Original appearance of PVOH pellets; (b) unplasticized extruded PVOH extrudate.

loss of water during heating in a DSC chamber, the remaining water content would not necessarily be the same as the original water content. So the actual melting temperature may be lower than what is presented here. Unless the DSC cell is sealed to prevent the sample from drying, this error will be unavoidable. There was also a shift in melting behaviors from the peak temperature in each curve with added water. Most likely, the surface area that dried locally during DSC heating must have shown higher melting behaviors. The gradual change in the water concentration seems to be reflected by the melting temperature curves.

Figure 5 shows an original appearance of PVOH pellets and an extruded sample of PVOH without water. Significant melt fracture and color change, both of which are associated with thermal degradation, were observed, because of the long exposure to a high temperature. The hydrogen bonds in the PVOH chains were ruptured. Without water, PVOH is in an unplasticized state that has a high degree of crystallinity and shows little or no thermoplasticity.³⁹ Therefore, water is a good PVOH plasticizer and plays a vital role in extrusion foaming. It decreases the melting point to avoid PVOH degradation and increases the PVOH chain mobility to facilitate processing at lower temperatures.

2.2. Effect of MFC on the Thermal Behavior of PVOH. MFC can influence polymer's crystallization kinetics. This affects cell nucleation and cell growth behaviors during the extrusion foaming^{34,40–43} of PVOH/MFC composites. Figure 6 shows the second heating and first cooling cycles of PVOH and PVOH/MFC composites without moisture effects. As previously noted, the degradation temperature of PVOH is close to its melting temperature.⁴⁴ During DSC characterization, there is a strong possibility that thermal degradation will occur. As suggested by Probst et al.,⁴⁵ even if there is no degradation during the first heating, it may occur during the second heating cycle, although Endo et al.⁴⁶ and Huang et al.⁴⁷ claimed that no significant degradation was detected using Fourier transform infrared (FTIR) spectroscopy and DSC. In brief, useful comparisons can be made from the second heating and the first cooling. The first heating was discarded to minimize the effect of the water. The specimens were heated from 30 °C to 205 °C at a rate of 10 °C/min and held at 205 °C for 2 min to eliminate any prior thermal history and minimize degradation. Then, they were cooled at a rate of 10 °C/min to 30 °C. Next, the samples were reheated to 205 °C and cooled to room temperature. PVOH and PVOH/MFC

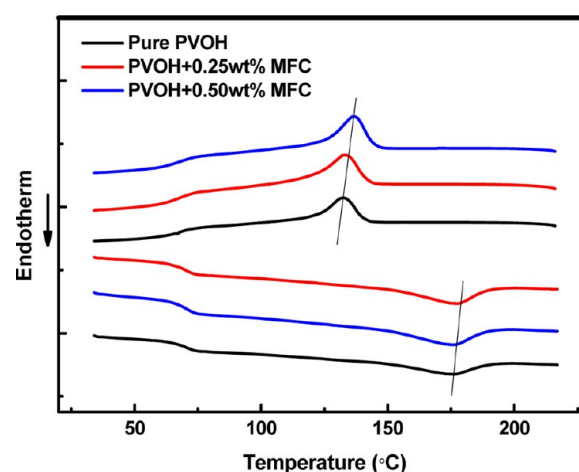


Figure 6. DSC thermograms of PVOH and PVOH/MFC composites.

composites melt over a large range from 150 to 200 °C. In the first cooling run, because of the motion and rearrangement of the PVOH molecules, the creation of various degrees of crystallinity is expected. The PVOH molecules also move sufficiently fast to form the nuclei needed for crystallization. On the other hand, the microsize to nanosize MFC can affect crystalline behavior because of its role as a crystal-nucleating agent, as Table 3 clearly shows. With MFC loaded, the

Table 3. DSC Results of Second Heating and First Cooling Curves

sample	T_m (°C)	ΔH (J/g)	X_c (%)	T_c (°C)
pure PVOH	176.1	8.81	5.87	132.6
PVOH + 0.25 wt % MFC	176.3	12.03	8.06	132.8
PVOH + 0.5 wt % MFC	177.7	12.08	8.07	136.6

crystallization temperature (T_c) became higher than it was for neat PVOH. With 0.5 wt % MFC, the PVOH's crystallization temperature was 4 °C higher. Furthermore, with increased MFC content, the melting temperature increased slightly. It can be concluded that PVOH compounded with MFC fibers affects its crystallization. In addition, the melt strength of PVOH increases significantly with increased MFC content, and this would increase the processing pressure.

The degree of crystallinity is shown in Table 3, and was calculated based on eq 2:

$$\chi_c = \frac{\Delta H_m}{w\Delta H_m^0} \quad (2)$$

where w is the weight fraction of the composites' PVOH, ΔH_m is the heat of fusion, and ΔH_m^0 is the heat of fusion of a 100% crystalline PVOH, which has a value of 150 J/g.⁴⁸ With increased MFC content, the crystallinity and crystallization temperature (T_c) both increased. Compared with neat PVOH, the crystallinity in this sample increased 2.5% with 0.25 wt % MFC. It is noteworthy that MFC fibers can also increase PVOH's crystal nucleation density. These small PVOH crystals can further contribute to cell nucleation.^{34,40–43,49} MFC fibers may also prevent large crystal formation in the restricted space.⁵⁰

Figure 7 shows the melting behavior of neat PVOH and PVOH/MFC composites with 20.5 wt % water. As the graphs

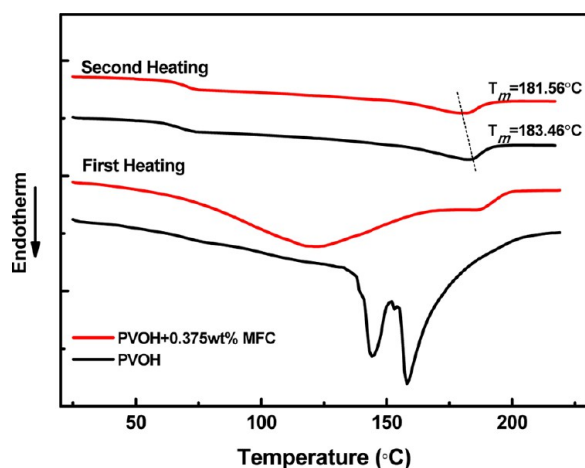


Figure 7. DSC thermograms of PVOH and PVOH/MFC composite with 20.5 wt % water.

show, both of these had a double melting peak in the first heating run, demonstrating that water affected PVOH melting. Although the initial amount of water was 20.5 wt %, the water concentration must have been initially nonuniform within each sample, because of the unavoidable local and partial drying of water from the PVOH. Furthermore, because of the difficulty in maintaining the constant water level within the PVOH sample, the DSC sample preparation process could have caused some drying of water. Finally, the drying that occurred during the DSC experiment must also have contributed to the outcome.

It was further observed that the melting behavior of the PVOH/MFC composites differed from that of the PVOH. First, the PVOH/MFC composites had a larger water content which affected the T_m . Also, the MFC addition enhanced crystal nucleation by acting as a crystal nucleating agent, which, with the help of water molecules, plasticized the PVOH chains. Therefore, the crystal morphology of the PVOH/MFC composites must have been different, and this must have affected the cell nucleation behaviors.

3. Cell Morphology of Foams Blown with scCO₂ and Water. PVOH/MFC composite foam experiments using a 0.05 and 0.1 wt % MFC master batch were carried out to identify the relationship between processing parameters and cell morphology. Cell nucleation behavior governs the final cell structure and the resultant foam properties. Therefore, we discuss cell nucleation behavior at the outset and then look at the final cell

morphology as a function of various processing and materials parameters.

3.1. Effects of Water and CO₂ on Cell Morphology. Figures 8a–d show extrusion-foamed samples at a high die temperature

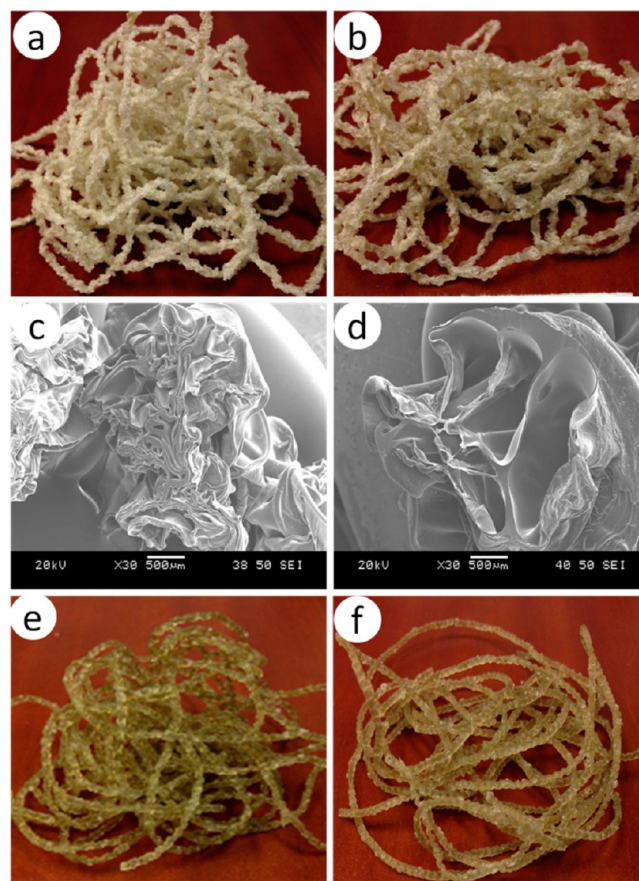


Figure 8. Foamed samples of PVOH with water as a plasticizer and blowing agent ((a) $T_{die} = 200$ °C and (b) $T_{die} = 190$ °C). SEM images of PVOH with water as a plasticizer and blowing agent ((c) $T_{die} = 200$ °C and (d) $T_{die} = 190$ °C). Water as a plasticizer and blowing agent of PVOH foamed sample ((e) $T_{die} = 160$ °C and (f) $T_{die} = 150$ °C).

and the SEM images of PVOH with 22.2 wt % water as a plasticizer and as a physical BA. It was reported that 22.7 wt % was an optimal water content for PVOH/water foaming.¹¹ Because water evaporation is strongly controlled by the melt temperature, it greatly affects the foaming behavior of PVOH/water compounds. At a high die temperature (180–200 °C), the extruded PVOH foam blown with water collapsed, and large cells were formed, as shown in Figures 8c and 8d. This is because water vaporizes quickly to form cells but condenses when cooled. Some water vapor may have diffused to the surface and transpired into the atmosphere. Similar results were reported in Wang's research.¹¹ At a low die temperature (≤ 160 °C), as Figures 8e and 8f show, there was almost no foaming. At low processing temperatures, the water remained trapped within the PVOH matrix. Thus, when only water was used as the physical BA, the nucleation during PVOH extrusion foaming was greatly weakened.

In PVOH/water extrusion foaming with scCO₂ and water as co-BAs, the content of either BA affects the foaming behavior. When the die temperature is higher than 170 °C, the foaming behavior is governed by water, which evaporates easily. At an elevated temperature, the PVOH has low melt strength and low

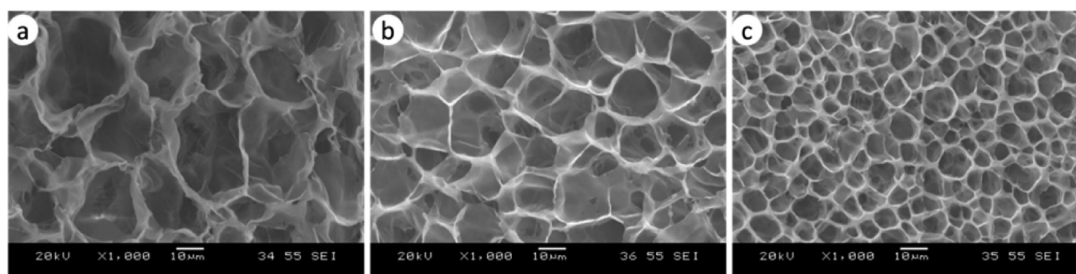


Figure 9. PVOH/MFC composite with 0.05 wt % MFC, 12.5 wt % water, and die temperature of 155 °C with various CO₂ contents: (a) 5 wt %, (b) 7 wt %, and (c) 9 wt %.

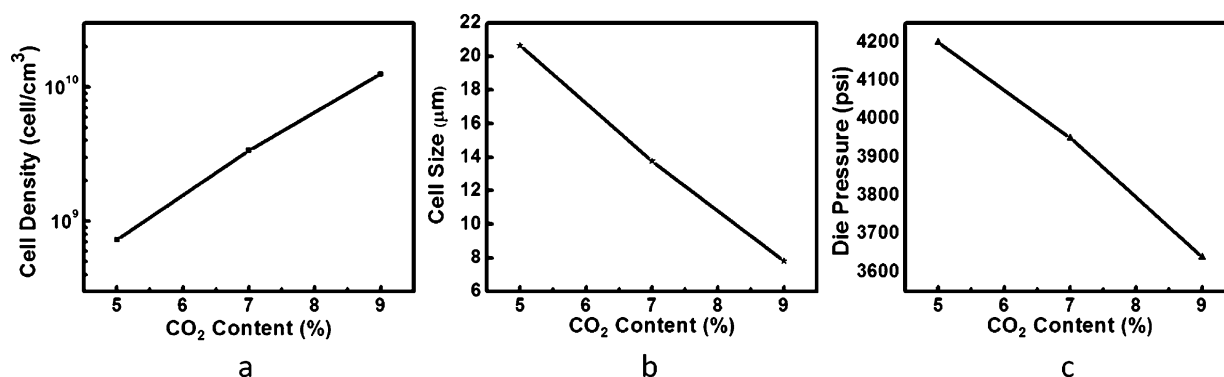


Figure 10. (a) Cell density, (b) cell size, and (c) die pressure of PVOH/MFC composite with 0.05 wt % MFC, 12.5 wt % water, and die temperature of 155 °C with various CO₂ contents.

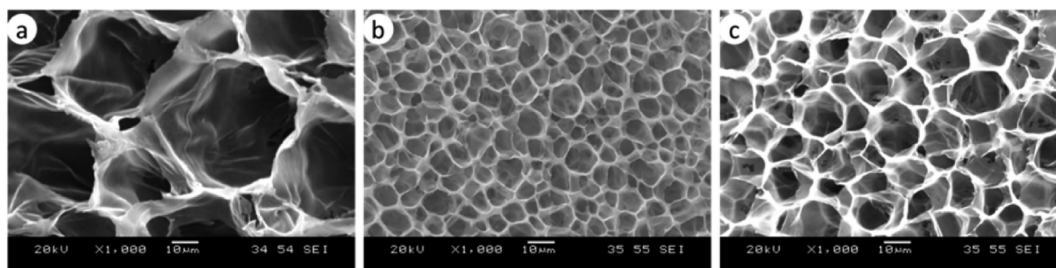


Figure 11. SEM images of PVOH and PVOH/MFC composites foam with 12.5 wt % water, 9 wt % CO₂, and a die temperature of 155 °C: (a) PVOH, (b) PVOH + 0.05 wt % MFC, and (c) PVOH + 0.1 wt % MFC.

viscosity. This leads to a low system pressure. Low melt strength and low system pressure cause cells to collapse and coalesce while scCO₂ escapes from the flexible foam. At low die temperatures, scCO₂ governs the foaming behavior. Water and scCO₂ are maintained within the PVOH matrix as a one-phase solution with a high system pressure. However, as water can reduce crystallinity and loosen the crystalline structure of PVOH, scCO₂ can easily diffuse throughout the PVOH matrix to form cell nucleation sites. When the die temperature was decreased, the cell size also decreased, and the cell coalescence phenomenon was suppressed.

Figure 9 shows the SEM micrographs of the samples foamed at a die temperature of 155 °C with 12.5 wt % water and 0.05 wt % MFC with varying CO₂ content. With increased scCO₂ content, the cell size decreased dramatically. This confirms that increased scCO₂ content in PVOH/MFC composites increased cell density, as shown in Figure 10 (see also Figure 12). Lee and Ramesh reported similar results earlier.^{24,51} Therefore, a higher scCO₂ content would be desirable; however, because of the back pressure needed to dissolve an injected CO₂ stream in the

polymer, the CO₂ content would be limited in extrusion foaming.⁵²

It seems that foaming PVOH and PVOH/MFC composites with scCO₂ and water can produce a good synergism. Water plasticizes the PVOH and thereby increases the low solubility of CO₂ while scCO₂ promotes cell density that cannot be achieved by using water alone.

3.2. Effect of MFC Content on Cell Morphology. During the foaming process of MFC-reinforced PVOH composites, MFC acts as an agent for heterogeneous nucleation and creates local stress/pressure variations that encourage cell nucleation.^{33,35} First, MFC is hydrophilic and has a large aspect ratio, which creates a large interfacial area that can generate numerous cell nucleation sites.⁵³ Added fiber could also improve cell nucleation, because of the local pressure variations and changes in interfacial tension. This behavior is calculated in eq 3:

$$R_{cr} = \frac{2\gamma_{lg}}{P_{bub, cr} - (P_{sys} + \Delta P_{local})} \quad (3)$$

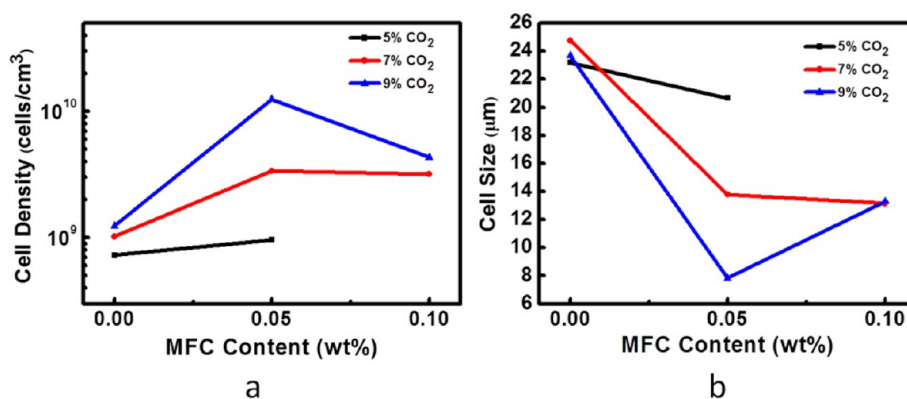


Figure 12. (a) Cell density and (b) cell size of PVOH and PVOH/MFC composites foam with 12.5 wt % water, 5, 7, and 9 wt % CO₂ and a die temperature of 155 °C.

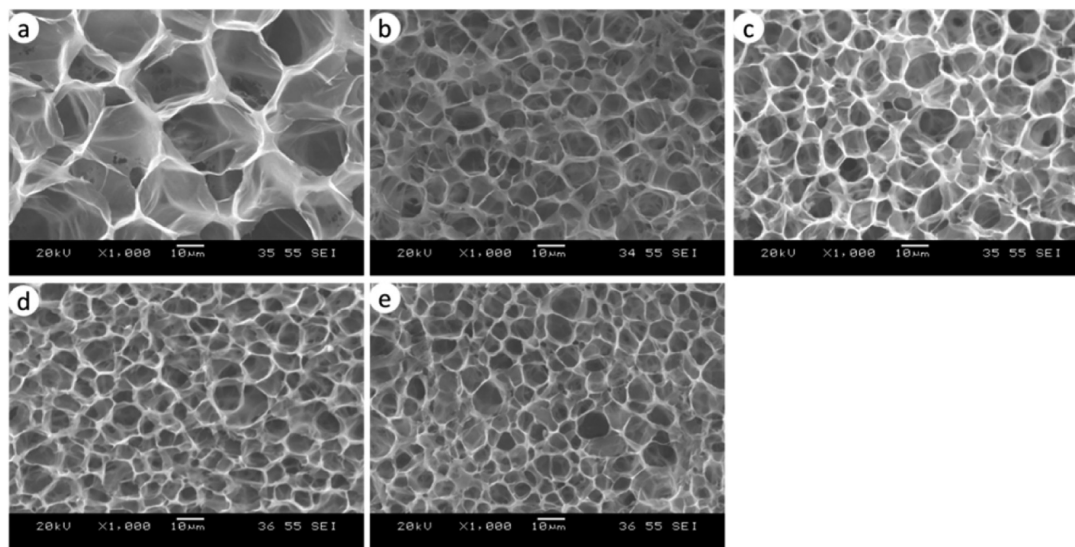


Figure 13. SEM images of PVOH/MFC composite foam with 0.05 wt % MFC, 12.5 wt % water, 9 wt % scCO₂, and various die temperatures: (a) 180 °C, (b) 170 °C, (c) 160 °C, (d) 150 °C, and (e) 140 °C.

where R_{cr} is the critical radius for cell nucleation, γ_{lg} the liquid–gas interfacial energy, $P_{bub,cr}$ the pressure inside a critical bubble, P_{sys} the system pressure, and ΔP_{local} the local pressure variation caused by the presence of the MFC fibers.^{33,35,54} In regions where tensile stresses exist, the critical radius would decrease. Consequently, the energy needed for cell nucleation would be reduced and cell nucleation would be promoted. In terms of mechanics, we found that dewetting of the polymer melt from the surface of the MFC, that is, cavity formation, can occur with a tensile stress. In addition, microvoids could pre-exist in the craters/crevices of the fibers that were in contact with the polymer melt due to contact angle constraints. As the critical radius decreased, the microvoids with sizes larger than the radius would grow spontaneously into nucleated cells.

Figure 11 shows the SEM micrographs of foamed samples with processing conditions of 12.5 wt % water and various MFC contents at a die temperature of 155 °C and in 9 wt % scCO₂. A uniform cell structure was found throughout all of the samples. In contrast to neat PVOH foams, cell size dramatically decreased with MFC loading. This indicated that effective MFC cell nucleation action had occurred within the PVOH. As Figure 12a shows, the highest cell density was 1.25×10^{10} cells/cm³ when the MFC content was at 0.05 wt % with 9 wt %

scCO₂. This was almost an order of magnitude higher than it was for neat PVOH. However, when we increased the MFC content to 0.1 wt %, the cell density was slightly decreased. This was most likely due to a combination of overloaded MFC, relative to its dispersing ability and the locally high concentration of water that evaporated from the MFC.^{55–57} Figure 12b shows that the average cell size ranged from 8 μm to 25 μm. The MFC played an important role as a nucleating agent during foaming, one that reduced the activation energy barrier to increase the cell nucleation rate. We also note that the MFC's influence on crystals affected cell nucleation. On the other hand, it can also enhance PVOH's melt strength and thereby suppress cell coalescence. Therefore, MFC, is an active parameter that can determine cell structure during extrusion foaming aided by water as a plasticizer. And, as discussed earlier, the optimal MFC content was 0.05 wt %.

3.3. Effect of Die Temperature on Cell Morphology. The SEM micrographs of foamed samples with 12.5 wt % water co-blown with 9 wt % scCO₂ and 0.05 wt % MFC at various die temperatures from 140 °C to 180 °C are shown in Figure 13. Uniform cell distribution was achieved and the cell size decreased as the die temperature decreased. In addition, Figure 14 shows that, with a decreased die temperature, the die

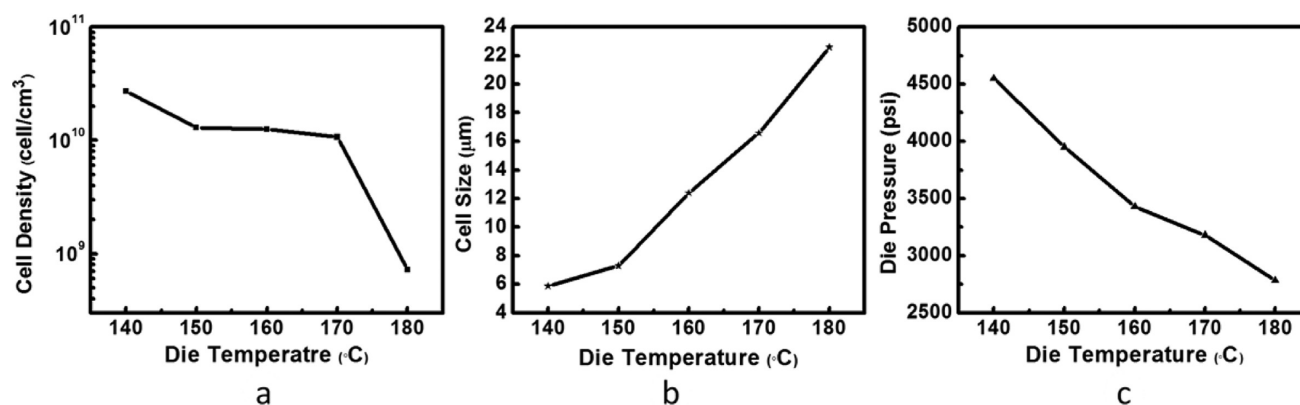


Figure 14. (a) Cell density, (b) cell size, and (c) die pressure of PVOH/MFC composite foam with 0.05 wt % MFC, 12.5 wt % water, 9 wt % CO₂, and various die temperatures.

pressure and cell density increased, and the cell size decreased. For example, the highest cell density was 2.7×10^{10} cells/cm³ with a die pressure of 4550 psi (31.4 MPa). This study shows that, at a high die temperature, the low melt strength of PVOH allowed for cell coalescence to occur when the nucleated cells grew and connected with each other. As the die temperature decreased, the coalescence phenomena also decreased, because of the increased PVOH melt strength and viscosity. At the same time, high die pressure can ensure the complete dissolution of the injected CO₂ and drive a great thermodynamic instability at the die exit.⁵⁸

In addition, a decreased die temperature can change the mobility of the molecular chains, and this affects the PVOH crystallization behaviors within the extruder and the die.^{34,40–43,59} These crystals affect both cell nucleation and cell growth foaming behaviors. The locally developed crystals will generate variations of the stresses around themselves, and this will greatly promote cell nucleation.^{34,42,60–62} Since the cell nucleation location is related to the nucleated crystals, the cell density can be increased by increasing the number of crystal nuclei using a crystal nucleating agent.

In addition, the crystals connect the polymer molecules and, therefore, the connected molecules will behave like long-chain branched materials. This will result in high melt strength and improved expanding ability, because of reduced cell coalescence and opening.⁴²

But an excessive degree of crystallinity will reduce the cell's expanding ability because the stiffness will be too great for its growth.⁵⁹ Therefore, an optimal degree of crystallization within the extruder is needed. In this context, an optimal degree of cooling will be required by a proper setting of the extrusion barrel and die temperatures.⁶³ In general, the crystallization kinetics can occur quite rapidly, especially with high shear and extensional rates extrusion foaming. And, for some materials, it may not be easy to control the crystallization kinetics within the extruder and the die. We observed that the temperature for foam processing of PVOH should be lower than 170 °C, and preferably it should be below 160 °C, based on the results shown in Figure 14.

CONCLUSIONS

Uniform cell structure and cell distribution with high cell density microcellular PVOH/MFC composite foams were obtained through tandem extrusion foaming with the use of scCO₂ and water as co-blowing agents. The effects of water and

MFC at different processing parameters on thermal behaviors and on cell morphology were shown. Several insights were gained from the study of these unique PVOH and PVOH/MFC composite systems. Water acted as a plasticizer and decreased the melting temperature. It also facilitated CO₂ processing and improved the extrusion foaming process. The MFC compounded with the PVOH matrix, and this affected melt strength and crystallinity. The MFC in PVOH also served as a cell nucleating agent and influenced cell nucleation and cell growth behaviors through crystallization. Cell density was increased with increased CO₂ content and decreased die temperature.

AUTHOR INFORMATION

Corresponding Authors

*E-mail: park@mie.utoronto.ca (C. B. Park).

*E-mail: qianli@zzu.edu.cn (Q. Li).

Notes

The authors declare no competing financial interest.

ACKNOWLEDGMENTS

The authors are grateful to the Kuraray Company for supplying PVOH and also to the industrial members of the Consortium of Cellular and MicroCellular Plastics (CCMCP) for their financial support of this project. The first author also acknowledges the China Scholarship Council for their support of her studies at the University of Toronto.

REFERENCES

- (1) Goodship, V.; Jacobs, D. K. In *Polyvinyl Alcohol: Materials, Processing and Applications*; Smithers Rapra Technology: Shawbury, Shrewsbury, Shropshire, U.K., 2009; Vol. 16, p 1.
- (2) Turbak, A. F.; Synder, F. W.; Sandberg, K. R. Microfibrillated cellulose, a new cellulose product: Properties, uses, and commercial potential. *J. Appl. Polym. Sci.* **1983**, *37*, 815–827.
- (3) Siró, I.; Plackett, D. Microfibrillated cellulose and new nanocomposite materials: A review. *Cellulose* **2010**, *17*, 459–494.
- (4) Chinga-Carrasco, G. Cellulose fibres, nanofibrils and microfibrils: The morphological sequence of MFC components from a plant physiology and fibre technology point of view. *Nanoscale Res. Lett.* **2011**, *6*, 417–424.
- (5) Boissard, C. I.; Bourban, P.-E.; Plummer, C. J. G.; Neagu, R. C.; Manson, J.-A. E. Cellular biocomposites from polylactide and microfibrillated cellulose. *J. Cell. Plast.* **2012**, *48*, 445–458.
- (6) Neagu, R. C.; Cuénoud, M.; Berthold, F.; Bourban, P.-E.; Gamstedt, E. K.; Lindström, M.; Manson, J.-A. E. The potential of

wood fibers as reinforcement in cellular biopolymers. *J. Cell. Plast.* **2012**, *48*, 71–103.

(7) Avella, M.; Cocca, M.; Errico, M. E.; Gentile, G. Polyvinyl alcohol biodegradable foams containing cellulose fibres. *J. Cell. Plast.* **2012**, *48*, 459–470.

(8) Kuboki, T. Foaming behavior of cellulose fiber-reinforced polypropylene composites in extrusion. *J. Cell. Plast.* **2013**, *50*, 113–128.

(9) Park, J. S.; Park, J. W.; Ruckenstein, E. A dynamic mechanical and thermal analysis of unplasticized and plasticized poly(vinyl alcohol)/methylcellulose blends. *J. Appl. Polym. Sci.* **2001**, *80*, 1825–1834.

(10) Lu, J.; Wang, T.; Drzal, L. T. Preparation and properties of microfibrillated cellulose polyvinyl alcohol composite materials. *Composites, Part A* **2008**, *39*, 738–746.

(11) Li, L.; Shi, H.; Shi, H. S.; Wang, Q. In *Preparation of Poly(vinyl alcohol) Foam through Thermal Processing using Water as Blowing Agent*, May 21–24, 2012; Polymer Processing Society Americas: Ontario, Canada, 2012.

(12) Guo, D.; Bai, S. B.; Wang, Q. A novel halogen-free flame retardant poly(vinyl alcohol) foam with intrinsic flame retardant characteristics prepared through continuous extrusion. *J. Cell. Plast.* **2014**, *0*, 1–19.

(13) Dexi, W.; Brooklyn, N. Y. Polyvinyl Alcohol Compound. U.S. Patent 5,804,653, Sept. 8, 1998.

(14) Guo, D.; Wang, Q.; Bai, S. Poly(vinyl alcohol)/melamine phosphate composites prepared through thermal processing: Thermal stability and flame retardancy. *Polym. Adv. Technol.* **2013**, *24*, 339–347.

(15) Wang, Q.; Li, L.; Shi, H.; Peng, X. Poly(vinyl alcohol) polar foam and its preparation method. Chin. Patent No. ZL200710049955.6, Sept. 10, 2010.

(16) Wang, Q.; Guo, D.; Bai, S.; Hua, Z. Halogen-free Flame Retardant Poly(vinyl alcohol) foam and its preparation method. Chin. Patent No. ZL201210033387.1, Jan. 22, 2014.

(17) Matuana, L. M.; Park, C. B.; Balatinez, J. J. Cell morphology and property relationships of microcellular foamed PVC/wood-fiber composites. *Polym. Eng. Sci.* **1998**, *38*, 1862–1872.

(18) Baldwin, D.; Suh, N. Viscoelastic behavior of microcellular plastics. In *Proceedings of SPE-ANTEC, Annual Technical Conference—Society of Plastics Engineers*; Society of Plastics Engineers: Newtown, CT, 1992; Paper No. 1503.

(19) Seeler, K. A.; Kumar, V. Tension-tension fatigue of microcellular polycarbonate: initial results. *J. Reinf. Plast. Compos.* **1993**, *12*, 359–376.

(20) Ito, M.; Kabumoto, A.; Okada, M.; Yoshida, N. Light reflecting plate. U.S. Patent 5,844,731, Dec. 1, 1998.

(21) Lee, Y. H.; Kuboki, T.; Park, C. B.; Sain, M. The effects of nanoclay on the extrusion foaming of wood fiber/polyethylene nanocomposites. *Polym. Eng. Sci.* **2011**, *51*, 1014–1022.

(22) Lee, Y. H.; Kuboki, T.; Park, C. B.; Sain, M.; Kontopoulou, M. The effects of clay dispersion on the mechanical, physical, and flame-retarding properties of wood fiber/polyethylene/clay nanocomposites. *J. Appl. Polym. Sci.* **2010**, *118*, 452–461.

(23) Ramesh, N. S.; Malwitz, N. Extrusion of Novel Water Soluble Biodegradable Foams. In *Proceedings of SPE-ANTEC, Annual Technical Conference—Society of Plastics Engineers*; Society of Plastics Engineers: Newtown, CT, 1995; Paper No. 55-2.

(24) Lee, S. T.; Park, C. B.; Ramesh, N. S. In *Polymeric Foams: Science and Technology*; CRC Press/Taylor and Francis: Boca Raton, FL, 2007; pp 171–180.

(25) Avella, M.; Cocca, M.; Errico, M.; Gentile, G. Biodegradable PVOH-based foams for packaging applications. *J. Cell. Plast.* **2011**, *47*, 271–281.

(26) Srithip, Y.; Turng, L.-S.; Sabo, R.; Clemons, C. Nanofibrillated cellulose (NFC) reinforced polyvinyl alcohol (PVOH) nanocomposites: Properties, solubility of carbon dioxide, and foaming. *Cellulose* **2012**, *19*, 1209–1223.

(27) Li, G.; Leung, S. N.; Hasan, M. M.; Wang, J.; Park, C. B.; Simha, R. A thermodynamic model for ternary mixture systems—Gas blends in a polymer melt. *Fluid Phase Equilib.* **2008**, *266*, 129–142.

(28) Wong, A.; Mark, L. H.; Hasan, M. M.; Park, C. B. The synergy of supercritical CO₂ and supercritical N₂ in foaming of polystyrene for cell nucleation. *J. Supercrit. Fluids* **2014**, *90*, 35–43.

(29) Sato, Y.; Yurugi, M.; Fujiwara, K.; Takishima, S.; Masuoka, H. Solubilities of carbon dioxide and nitrogen in polystyrene under high temperature and pressure. *Fluid Phase Equilib.* **1996**, *125*, 129–138.

(30) Sato, Y.; Fujiwara, K.; Takikawa, T.; Takishima, S.; Masuoka, H. Solubilities and diffusion coefficients of carbon dioxide and nitrogen in polypropylene, high-density polyethylene, and polystyrene under high pressures and temperatures. *Fluid Phase Equilib.* **1999**, *162*, 261–276.

(31) Li, G.; Wang, J.; Park, C.; Simha, R. Measurement of gas solubility in linear/branched PP melts. *J. Polym. Sci., Part B* **2007**, *45*, 2497–2508.

(32) Hasan, M. M.; Li, Y. G.; Li, G.; Park, C. B.; Chen, P. Determination of solubilities of CO₂ in linear and branched polypropylene using a magnetic suspension balance and a PVT apparatus. *J. Chem. Eng. Data* **2010**, *55*, 4885–4895.

(33) Wong, A.; Park, C. B. The effects of extensional stresses on the foamability of polystyrene–talc composites blown with carbon dioxide. *Chem. Eng. Sci.* **2012**, *75*, 49–62.

(34) Wong, A.; Guo, Y.; Park, C. B. Fundamental mechanisms of cell nucleation in polypropylene foaming with supercritical carbon dioxide—Effects of extensional stresses and crystals. *J. Supercrit. Fluids* **2013**, *79*, 142–151.

(35) Wong, A.; Wijnands, S. F.; Kuboki, T.; Park, C. B. Mechanisms of nanoclay-enhanced plastic foaming processes: effects of nanoclay intercalation and exfoliation. *J. Nanopart. Res.* **2013**, *15*, 1–15.

(36) Leung, S. N.; Wong, A.; Guo, Q.; Park, C. B.; Zong, J. H. Change in the critical nucleation radius and its impact on cell stability during polymeric foaming processes. *Chem. Eng. Sci.* **2009**, *64*, 4899–4907.

(37) Leung, S. N.; Wong, A.; Wang, L. C.; Park, C. B. Mechanism of extensional stress-induced cell formation in polymeric foaming processes with the presence of nucleating agents. *J. Supercrit. Fluids* **2012**, *63*, 187–198.

(38) Assender, H. E.; Windle, A. H. Crystallinity in poly(vinyl alcohol). 1. An X-ray diffraction study of atactic PVOH. *Polymer* **1998**, *39*, 4295–4302.

(39) Marten, F. L.; Famili, A.; Nangeroni, J. F. Extrudable polyvinyl alcohol compositions. Eur. Patent No. EP 0415357 B2, June 5, 1999.

(40) Mihai, M.; Huneault, M. A.; Favis, B. D.; Li, H. Extrusion Foaming of Semi-Crystalline PLA and PLA/Thermoplastic Starch Blends. *Macromol. Biosci.* **2007**, *7*, 907–920.

(41) Mihai, M.; Huneault, M. A.; Favis, B. D. Crystallinity development in cellular poly (lactic acid) in the presence of supercritical carbon dioxide. *J. Appl. Polym. Sci.* **2009**, *113*, 2920–2932.

(42) Wang, J.; Zhu, W.; Zhang, H.; Park, C. B. Continuous processing of low-density, microcellular poly(lactic acid) foams with controlled cell morphology and crystallinity. *Chem. Eng. Sci.* **2012**, *75*, 390–399.

(43) Tabatabaei, A.; Barzegari, M. R.; Nofar, M.; Park, C. B. In-situ visualization of polypropylene crystallization during extrusion. *Polym. Test.* **2014**, *33*, 57–63.

(44) Tang, X.; Alavi, S. Recent advances in starch, polyvinyl alcohol based polymer blends, nanocomposites and their biodegradability. *Carbohydr. Polym.* **2011**, *85*, 7–16.

(45) Probst, O.; Moore, E. M.; Resasco, D. E.; Grady, B. P. Nucleation of polyvinyl alcohol crystallization by single-walled carbon nanotubes. *Polymer* **2004**, *45*, 4437–4443.

(46) Endo, R.; Amiya, S.; Hikosaka, M. Conditions for melt crystallization without thermal degradation and equilibrium melting temperature of atactic poly(vinyl alcohol). *J. Macromol. Sci. B* **2003**, *42*, 793–820.

(47) Huang, H.; Gu, L.; Ozaki, Y. Non-isothermal crystallization and thermal transitions of a biodegradable, partially hydrolyzed poly(vinyl alcohol). *Polymer* **2006**, *47*, 3935–3945.

(48) Finch, C. A. *Poly(vinyl alcohol) developments*; John Wiley & Sons: London, 1992.

- (49) Reignier, J.; Tatibouët, J.; Gendron, R. Batch foaming of poly (ϵ -caprolactone) using carbon dioxide: Impact of crystallization on cell nucleation as probed by ultrasonic measurements. *Polymer* **2006**, *47*, 5012–5024.
- (50) Guo, G.; Wang, K.; Park, C.; Kim, Y.; Li, G. Effects of nanoparticles on the density reduction and cell morphology of extruded metallocene polyethylene/wood fiber nanocomposites. *J. Appl. Polym. Sci.* **2007**, *104*, 1058–1063.
- (51) Lee, S. T.; Ramesh, N. S.; Campbell, G. A. Temperature Effects on Thermoplastic Foam Sheet Formation. In *Proceedings of SPE-ANTEC, Annual Technical Conference—Society of Plastics Engineers*; Society of Plastics Engineers: Newtown, CT, 1993.
- (52) Xu, X.; Park, C. B.; Xu, D.; Pop-Iliev, R. Effects of die geometry on cell nucleation of PS foams blown with CO₂. *Polym. Eng. Sci.* **2003**, *43*, 1378–1390.
- (53) Kuboki, T.; Lee, Y. H.; Park, C. B.; Sain, M. Mechanical properties and foaming behavior of cellulose fiber reinforced high-density polyethylene composites. *Polym. Eng. Sci.* **2009**, *49*, 2179–2188.
- (54) Wong, A.; Park, C. B. A visualization system for observing plastic foaming processes under shear stress. *Polym. Test.* **2012**, *31*, 417–424.
- (55) Matuana, L. M.; Mengeloglu, F. Manufacture of rigid PVC/wood-flour composite foams using moisture contained in wood as foaming agent. *J. Vinyl Addit. Technol.* **2002**, *8*, 264–270.
- (56) Rizvi, G.; Matuana, L. M.; Park, C. B. Foaming of PS/wood fiber composites using moisture as a blowing agent. *Polym. Eng. Sci.* **2000**, *40*, 2124–2132.
- (57) Rizvi, G. M.; Park, C. B.; Lin, W. S.; Guo, G.; Pop-Iliev, R. Expansion mechanisms of plastic/wood-flour composite foams with moisture, dissolved gaseous volatiles, and undissolved gas bubbles. *Polym. Eng. Sci.* **2003**, *43*, 1347–1360.
- (58) Park, C. B.; Behraves, A. H.; Venter, R. D. Low density microcellular foam processing in extrusion using CO₂. *Polym. Eng. Sci.* **1998**, *38*, 1812–1823.
- (59) Naguib, H. E.; Park, C. B.; Song, S.-W. Effect of Supercritical Gas on Crystallization of Linear and Branched Polypropylene Resins with Foaming Additives. *Ind. Eng. Chem. Res.* **2005**, *44*, 6685–6691.
- (60) Zhai, W.; Ko, Y.; Zhu, W.; Wong, A.; Park, C. B. A study of the crystallization, melting, and foaming behaviors of polylactic acid in compressed CO₂. *Int. J. Mol. Sci.* **2009**, *10*, 5381–5393.
- (61) Zhai, W.; Kim, Y.-W.; Jung, D. W.; Park, C. B. Steam-Chest Molding of Expanded Polypropylene Foams. 2. Mechanism of Interbead Bonding. *Ind. Eng. Chem. Res.* **2011**, *50*, 5523–5531.
- (62) Guo, Y.; Hossieny, N.; Chu, R. K.; Park, C. B.; Zhou, N. Critical processing parameters for foamed bead manufacturing in a lab-scale autoclave system. *Chem. Eng. J.* **2013**, *214*, 180–188.
- (63) Naguib, H. E.; Park, C. B.; Reichelt, N. Fundamental foaming mechanisms governing the volume expansion of extruded polypropylene foams. *J. Appl. Polym. Sci.* **2004**, *91*, 2661–2668.